

RESEARCH

Open Access



Value of serum LncRNA KIF9-AS1 combined with CT signs in the diagnosis of benign and malignant early pulmonary nodules and its correlation with prognosis

Huichao Wu^{1†}, Jian Liu^{2†}, Zhongjun Jing³, Zihua Qi⁴, Xianjun Ma⁵, Junying Zhao^{6*} and Laichong Huang^{7*}

Abstract

Background Early screening for lung cancer and early treatment of malignant pulmonary nodules (PNs) contribute a lot to reducing lung cancer mortality. Whether the highly expressed lncRNA KIF9-AS1 in multiple malignancies is associated with the development of malignant PNs is not clear. This study focused on the diagnosis and prognosis value of KIF9-AS1 in PNs patients.

Methods The study population included 101 individuals with benign PNs and 172 patients diagnosed with malignant PNs. The expression of KIF9-AS1 was analyzed by qRT-PCR. The receiver operator characteristic (ROC) curve was plotted to evaluate the diagnostic performance while the Kaplan-Meier curve and multivariate Cox regression analysis were employed for prognosis. Correlation assessment was accomplished by Pearson correlation analysis.

Results Differentiated expression of KIF9-AS1 was found in benign and malignant PNs groups. The expression of KIF9-AS1 was positively associated with carcinoembryonic antigen (CEA) and cytokeratin 19 fragments 21 – 1 (CYFRA21-1). KIF9-AS1 presented high accuracy in distinguishing malignant PNs from benign PNs, especially combined with computed tomography (CT). The expression level of KIF9-AS1, and nodule diameter were independent risk factors of poor prognosis.

Conclusions Assessment of serum KIF9-AS1 level contributed to clinical diagnosis and prognosis of malignant PNs and also improved the diagnostic value of CT.

Keywords KIF9-AS1, Pulmonary nodules, Diagnosis, Prognosis

[†]Huichao Wu and Jian Liu should be considered joint first author.

*Correspondence:

Junying Zhao

zhaojunyingdr123@163.com

Laichong Huang

Huanglaichong25@163.com

¹Department of Emergency, The First People's Hospital of Jiashan, Jiashan 314100, Zhejiang, China

²Department of Traditional Chinese Medicine for Pulmonology, China-Japan Friendship Hospital, Beijing 100029, China

³Department of Medical Imaging, Hospital of University of Jinan, Jinan 250022, Shandong, China

⁴Department of Medical Imaging, Qilu Hospital of Shandong University, Jinan 250012, Shandong, China

⁵Department of Blood Transfusion, Qilu Hospital of Shandong University, Jinan 250012, Shandong, China

⁶Department of Pharmacy, Hospital of University of Jinan, No. 336, Nanxinshuang West Road, Shizhong District, Jinan 250022, Shandong, China

⁷Department of Radiology and Imaging, Ruian People's Hospital, No. 108, Wansong Road, Ruian 325200, Zhejiang, China



Background

Pulmonary nodules (PNs) are lesions found in the lung with a maximum diameter of no more than 30 mm [1]. With the wide application and the increased sensitivity of low-dose computed tomography (CT), an increasing number of indeterminate PNs have been visualized. PNs were mainly divided into pure ground glass nodules, mixed ground glass nodules and solid nodules [2]. Although most of them are benign, some are malignant, known as lung cancer. The probability of malignancy has been reported to be close to 63% for the mixed ground glass nodules, with pure ground glass nodules accounting for 18% [3]. Additionally, solid nodules had the lowest probability of deterioration (7%) [3–5], but it was related to the worst prognosis [6]. In addition, a meta-analysis covering 185 countries in 2018 reports that lung cancer is often diagnosed at the advanced stage, with a 5-year survival rate of 17.4% [7]. Fortunately, it has been reported that early screening for lung cancer and early treatment of malignant PNs contribute to reducing lung cancer mortality by about 20% [8]. Therefore, the early detection of benign and malignant PNs plays an important role in early identification, treatment and improving survival rate of lung cancer.

Long non-coding RNAs (lncRNAs) have been considered as pivotal regulators of gene expression. Various lncRNAs have been shown to be related to lung cancer or PNs. An analysis of expression profiles of lung cancer plasma indicates that a large number of lncRNAs are differentially expressed in patients [9]. The serum lncRNA THRIL is found to be up-regulated in malignant PNs and accelerates the progression of lung cancer [10]. A report concerning non-small cell lung cancer (NSCLC) has demonstrated that highly expressed lncRNA CALML3-AS1 promotes tumor growth and liver metastasis [11]. The lncRNA XLOC-009167 has been confirmed to have important clinical predictive significance in lung cancer patients [12]. In recent years, a series of reports have shown that lncRNA KIF9-AS1 plays a significant role in various malignant tumors. For instance, the KIF9-AS1 has been reported to be increased in hepatocellular carcinoma tissues and facilitates the cell proliferation and migration [13]. Similar situation is also shown in patients with nasopharyngeal carcinoma [14]. In addition, it has also been shown that the KIF9-AS1 is implicated in the progression of renal cell carcinoma [15]. Therefore, the abnormal expression of KIF9-AS1 may involve in the growth of PNs.

This study focused on the different expression of KIF9-AS1 in benign and malignant PNs and explored the clinical value in the diagnosis of malignant PNs and in the prognosis evaluation of patients with malignant PNs.

Methods

Study population

The study population from January 2021 to December 2023 included 101 individuals with benign PNs and 172 patients diagnosed with malignant PNs from Hospital of University of Jinan. Pathologically, malignant PNs refer to primary lung cancer, including NSCLC and small cell lung cancer. The benign PNs mainly refer to the local space-occupying lesion of the lung, including Pulmonary tuberculosis, inflammatory calcified nodules, benign tumors of the lung such as hamartoma and fibroma. Their age ranged from 25 to 80 years. Chest CT showed at least 1 pulmonary nodule with a maximum diameter of ≤ 30 mm. Patients with clear PNs pathological reports and complete case data were included. Patients who had received antineoplastic therapy before enrollment or had a history of lung cancer, were excluded. PNs were pathologically diagnosed as lung metastases from other tumors were also not considered. In addition, patients with severe complications were also not taken into consideration. Besides, cases with missing data were excluded from the study. Before pathological confirmation, benign and malignant pulmonary nodules were initially identified and classified by a variety of methods, including clinical characteristics, serological examination for tumor markers and imaging examination of CT. The clinical characteristics included previous physical examination results, and related symptoms such as chest pain, cough, cough and sputum, chest tightness, fever, etc. This study obtained the approval of the Ethics Committee (NCT04052620) and informed consent of all enrolled patients.

Chest CT

A CT scanner was used for chest CT. The scanning ranged from lung apex to 2–3 cm below the lower lateral costophrenic Angle. Scanning was performed using the breath-hold method after deep inspiration and a supine position with hands up was required for patients. The tube voltage was set at 120 kV and adjusted according to the body mass index of patients, while the tube current was no more than 50 mAs. The resolution was set at 512×512 pixels and the pitch was 1 matrix. The iterative reconstruction algorithm was used to reduce image noise. The thickness of the reconstructed slices was 0.625–1.250 mm, and there was 20–30% overlap between layers. Two radiologists with more than 5 years of work experience analyzed and organized the images. The size, air bronchogram and density of nodules were analyzed.

qRT-PCR

Before medical or surgical treatment, the peripheral blood samples were obtained. After being left to stand

for half to an hour, the blood samples were centrifuged at 4000 rpm for 15 min, thus obtaining the serum samples, which were stored at -80°C . RNA extraction was performed by Trizol (Invitrogen). The RNA purity and integrity were assessed by the ratio of A260/A280 with a NanoDrop. The reverse transcription kit (Takara) was used to obtain cDNAs for later quantitative PCR. The expression of KIF9-AS1 (F: 5'-AGTCCTTCCCATTTCACAGGG-3', R: 5'-GCCCTCTTCTTCCTCC ACAT-3') was analyzed by $2^{-\Delta\Delta\text{Ct}}$ methods with GAPDH (F: 5'-TGTTCGTCATGGGTGTGAAC-3', R: 5'-ATGGCATGGACTGTGGTCAT-3') as the internal reference.

Detection for tumor markers

ELISA assay (enzyme-linked immunosorbent assay) with commercial kits was employed for the detection of serum tumor markers including CEA (CanAg CEA EIA kit), CA125 (RayBio CA125 ELISA kit), NSE (DRG NSE kit), and CYFRA21-1 (MyBioSource CYFRA21-1 kit). All procedures were performed following the instructions of above kits.

Follow-up

172 patients with malignant PNs were followed up after medical or surgical treatment. The follow-up period was 5 years by means of phone calls, inspections after treatment, or in-person visits. The patient's condition was recorded according to follow-up results.

Statistical analysis

GraphPad Prism 7.0 and SPASS 23.0 were used for Data analysis and processing. Results were presented as mean \pm SD. Difference analysis between groups was by Student's t-tests. The ROC and Kaplan-Meier curves were

plotted to assess the diagnostic and prognostic capability of KIF9-AS1. Pearson correlation analysis was used for evaluating the association between KIF9-AS1 and tumor markers. Risk factors analysis was accomplished by logistic regression, in which indicators showing statistically significant difference were included. $P < 0.05$ means statistical difference.

Results

Basic characteristics of study objects

101 individuals with benign PNs and 172 patients diagnosed with malignant PNs took part in this study. The basic information including average age, gender, smoking history, extra-lung cancer history, family cancer history, nodule density, nodule diameter and air bronchogram were analyzed. The statistics showed differences in extra-lung cancer history, nodule density and nodule diameter. In general, patients in malignant PNs group presented a higher proportion of extra-lung cancer history (79.65%, $P = 0.001$), higher nodule density (-601.78 ± 130.80 , $P = 0.001$) and longer nodule diameter (20.73 ± 6.04 , $P < 0.001$), by comparison with benign PNs group. Detailed information was exhibited in Table 1.

Expression level of lncRNA KIF9-AS1 in patients

The relative expression of lncRNA KIF9-AS1 in benign and malignant PNs was assessed by quantitative PCR, after conventional RNA extraction and reverse transcription. Compared to the benign PNs group, the lncRNA KIF9-AS1 presented an obviously increased expression in the malignant PNs group (Fig. 1, $P < 0.001$). This aberrant increase implied the relevance of lncRNA KIF9-AS1 to malignant PNs.

Table 1 Clinical characteristics of the study population

Characteristics	Benign PNs (n = 101)	Malignant PNs (n = 172)	P value
Age, years	59.60 \pm 8.66	61.77 \pm 11.02	0.107
Gender, n (%)			0.211
Male	42(41.58%)	58 (33.72%)	
Female	59 (58.42%)	114 (66.28%)	
Smoking history, n (%)			0.409
No	87 (86.14%)	142 (82.56%)	
Yes	14 (13.86%)	30 (17.44%)	
Extra-lung cancer history, n (%)			0.001
No	96 (95.05%)	137 (79.65%)	
Yes	5 (4.95%)	35 (20.35%)	
Family cancer history, n (%)			0.605
No	92 (91.09%)	153 (88.95%)	
Yes	9 (8.91%)	19 (11.05%)	
Nodule density, HU	-516.197 \pm 232.52	-601.78 \pm 130.80	0.001
Air bronchogram, n (%)	65 (64.35%)	128 (74.41%)	0.056
Nodule diameter, mm	12.02 \pm 5.08	20.73 \pm 6.04	<0.001

Note: PNs, pulmonary nodules

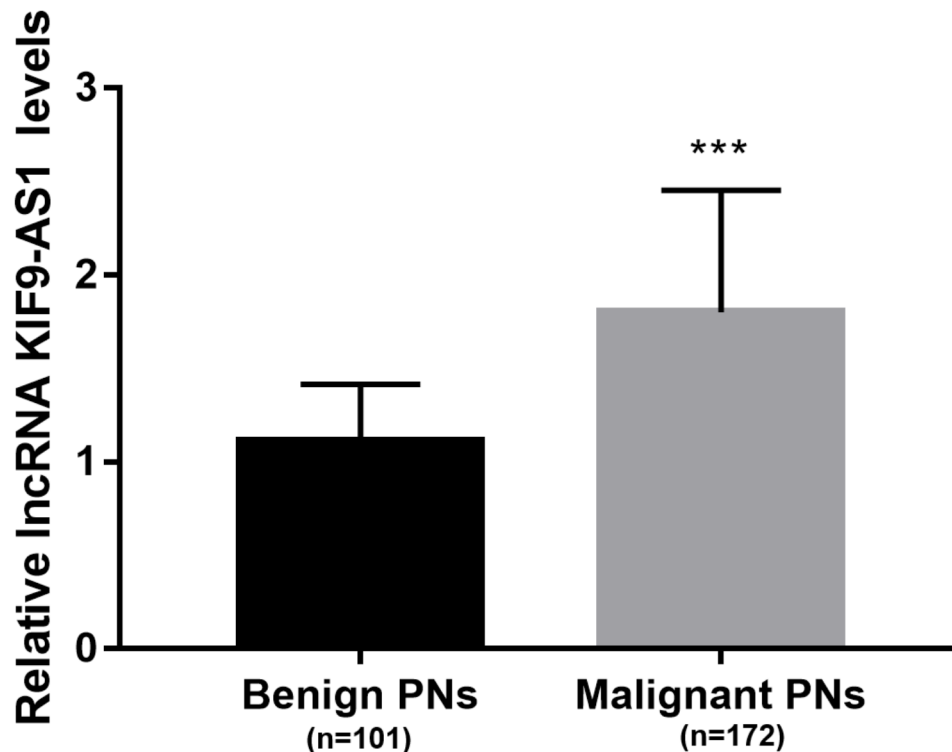


Fig. 1 The relative expression of lncRNA KIF9-AS1 in benign PNs group and malignant PNs group. The lncRNA KIF9-AS1 presented an obviously increased expression in the malignant PNs group ($P < 0.001$)

Relative expression of tumor markers and association with lncRNA KIF9-AS1

The clinical lung cancer-related serum markers were detected. The concentration of carcinoembryonic antigen (CEA), cytokeratin 19 fragments 21–1 (CYFRA21-1), carbohydrate antigen 125 (CA125) and neuron-specific enolase (NSE) were all elevated in malignant PNs. The elevation of CA125 and NSE was not prominent compared with that in the benign PNs group (Fig. 2B and D). However, the CEA and CYFRA21-1 were significantly elevated in malignant PNs (Fig. 2A and C). Considering the obvious increase of lncRNA KIF9-AS1 in malignant PNs, we assessed its association with differently expressed tumor markers. Data showed that the expression of lncRNA KIF9-AS1 was positively correlated with CEA (Fig. 2E, $r = 0.7566$, $P < 0.0001$) and CYFRA21-1 (Fig. 2E, $r = 0.7109$, $P < 0.0001$).

Diagnostic performance of lncRNA KIF9-AS1 with CT

Based on the different expression level between groups, the ROC curve was applied to evaluate its diagnosability in distinguishing patients with malignant PNs from those with benign PNs. The area under the curve was 0.835 while the sensitivity and specificity were 73.26% and 86.52% respectively (Fig. 3A). As both nodule diameter and density showed differences between the two groups, ROC curves were also drawn to evaluate their

diagnostic performance. For nodule diameter, the area under the curve was 0.847 with the sensitivity of 73.84% and specificity of 82.18% (Fig. 3B). For nodule density, the area under the curve was 0.605 with the sensitivity of 88.37% and specificity of 35.64% (Fig. 3B). The combined ROC curve exhibited optimal diagnosability as shown in Fig. 3C. The area under the combined ROC curve was 0.956 while the sensitivity and specificity were 80.80% and 96.00%, respectively. Thus it can be seen that the prediction model of a single factor, such as KIF9-AS1, nodule diameter or nodule density was not ideal. In contrast, the three-factor combined model showed satisfactory sensitivity and specificity.

Prognostic value of lncRNA KIF9-AS1

Since the highly expressed lncRNA KIF9-AS1 had a good diagnostic performance in identifying patients with malignant early PNs and was strongly correlated with tumor markers CEA and CYFRA21-1, further analysis was focused on its possible correlation with prognostic of early PNs. Five-year follow-up was performed in patients with malignant PNs. These patients were divided into the Low KIF9-AS1 group ($n = 82$) and the High KIF9-AS1 group ($n = 90$) based on the average KIF9-AS1 level. Statistics showed 32 individual from the low KIF9-AS1 group and 58 individuals from the high KIF9-AS1 group died during follow-up period. Kaplan-Meier

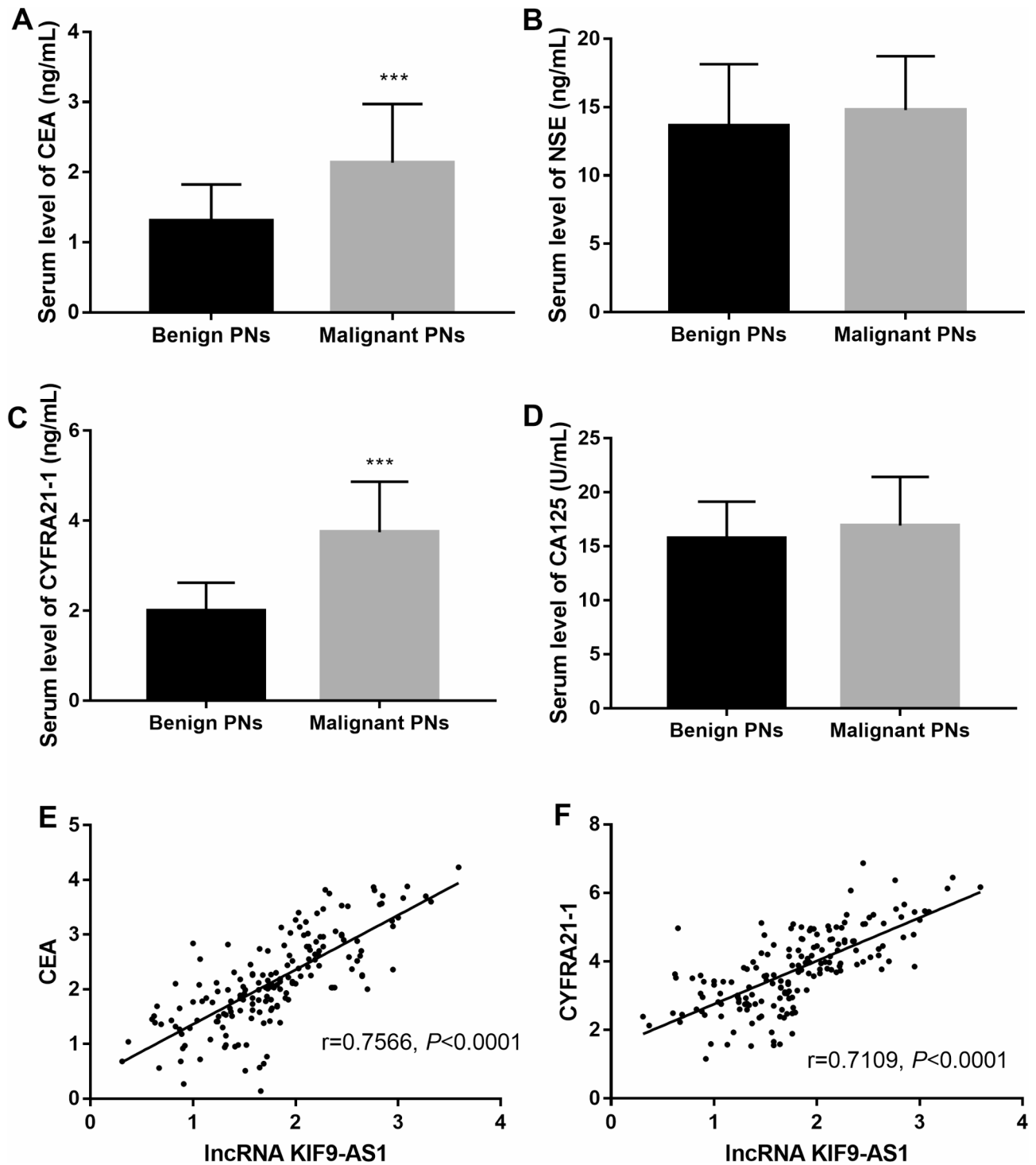


Fig. 2 Relative expression of tumor markers and association with lncRNA KIF9-AS1 in benign and malignant PNs groups. **(A)** Relative expression level of serum CEA ($P < 0.001$). **(B)** Relative expression level of serum NSE. **(C)** Relative expression level of serum CYFRA21-1 ($P < 0.001$). **(D)** Relative expression level of serum CA125. **(E)** Pearson correlation analysis between serum CEA and lncRNA KIF9-AS1. **(F)** Pearson correlation analysis between serum CYFRA21-1 and lncRNA KIF9-AS1. Relative expression of tumor markers were elevated in malignant PNs compared to the benign PNs. The levels of serum CEA and CYFRA21-1 were significantly elevated in malignant PNs. The expression of lncRNA KIF9-AS1 was positively correlated with CEA and CYFRA21-1

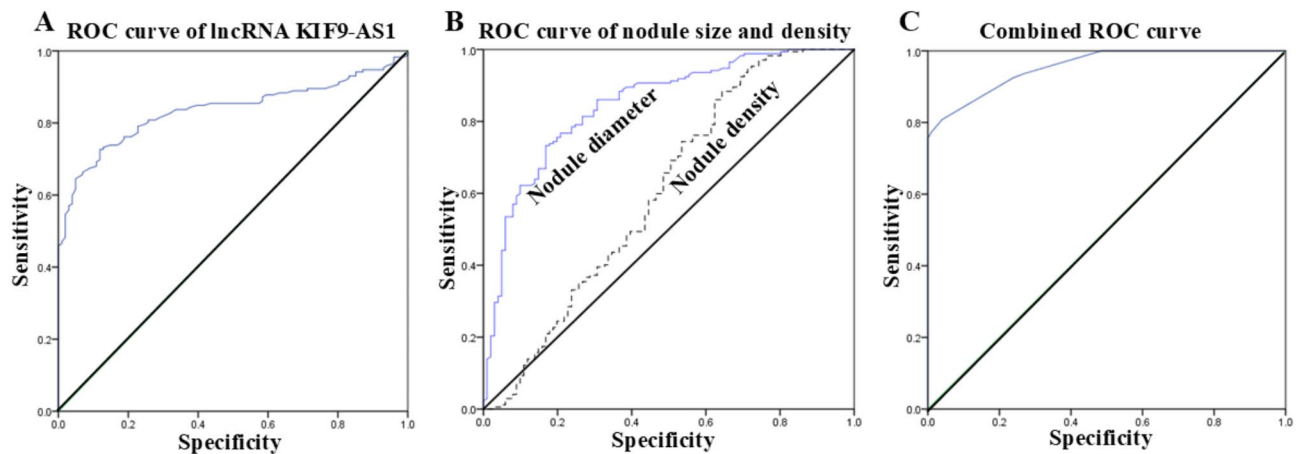


Fig. 3 The diagnostic performance of lncRNA KIF9-AS1 combined with CT. **(A)** The receiver operator characteristic (ROC) curve of lncRNA KIF9-AS1 (sensitivity = 73.26%, specificity = 86.52%, AUC = 0.835). **(B)** ROC curve of nodule diameter (sensitivity = 73.84%, specificity = 82.18%, AUC = 0.847) and nodule density (sensitivity = 88.37%, specificity = 35.64%, AUC = 0.605). **(C)** Combined ROC curve (sensitivity = 80.80%, specificity = 96.00%, AUC = 0.956)

curve showed that significantly reduced survival rate was exhibited in high KIF9-AS1 group compared to the low KIF9-AS1 group (Fig. 4, $P=0.008$). Therefore, highly expressed lncRNA KIF9-AS1 was associated with poor prognosis. Further multivariate Cox regression analysis demonstrated that the nodule diameter (HR = 1.642, 95% CI: 1.032–2.613, $P=0.036$) and lncRNA KIF9-AS1 (HR = 1.805, 95% CI: 1.141–2.855, $P=0.012$) were independent risk factors in patients with malignant PNs (Table 2).

Discussion

With the wide application and the increased sensitivity of low-dose computed tomography (CT), an increasing number of indeterminate PNs have been visualized. Early resection of malignant PNs is considered to be beneficial to the prognosis of patients [16]. However, the accuracy of chest CT still needs to be improved, especially for PNs with atypical morphological and hemodynamic characteristics [10], and relevant tumor markers such as CEA also have their limitations in clinical diagnosis. Therefore, it is still necessary to find new tumor markers. In this study, we found that significantly increased serum KIF9-AS1 contributed to clinical diagnosis and prognosis of malignant PNs. Additionally, it also improved the diagnostic value of CT.

lncRNAs are reported to be closely related to disease. High expression of lncRNA MIAT is thought to accelerate the progression of pneumonia [17]. The significantly increased LUCAT1 in NSCLC, is related to tumor size and is identified as a potential poor prognostic biomarker [18]. In this study, we found that the serum KIF9-AS1 was obviously higher in malignant PNs patients compared to that in benign PNs individuals. Furthermore, the nodule diameter in the malignant PNs group was more longer. Similar effects can also be observed in existing reports.

KIF9-AS1 is upregulated in both patients and mouse models of inflammatory bowel disease [19]. The KIF9-AS1 is reported to be upregulated in hepatocellular carcinoma patients and data from mice model demonstrates that KIF9-AS1 promotes the carcinoma development [13]. Further analysis showed that KIF9-AS1 exerted its effects through promoting cell proliferation, migration, and inhibiting apoptosis. Our data implied that the abnormal expression of KIF9-AS1 might be closely related to the malignant PNs by regulating above biological process.

By measuring tumor markers in the patient's blood, we found that the level of CEA and CYFRA21-1 were significantly elevated in the malignant PNs group. The CEA has been considered as a risk factor for prognosis in NSCLC [20] and can be used for postoperative monitoring [21]. CYFRA 21-1 is reported as a biomarker for early screening of lung cancer [22]. It has also been reported that CEA and CYFRA 21-1 can be used as serum markers for lung cancer diagnosis either in combination or alone [23]. In addition, the prognostic value of both markers in lung cancer has also been reported [24]. The positive correlation of KIF9-AS1 with CEA and CYFRA 21-1 were also demonstrated by Pearson correlation analysis in our study, which was another supporting evidence for our above findings. The increased expression of CEA and CYFRA21-1 indicated the increased malignancy of pulmonary nodules, which might be caused by the abnormal increase of KIF9-AS1. We expect to address it in subsequent studies although the potential association of them has not been confirmed in current reports. Specific lncRNA are found to be promising biomarkers for cancer diagnosis and prognosis. LINC02159 plays an oncogenic role in NSCLC and is regarded as a potential diagnostic marker [25]. Elevated HOTAIR has been confirmed to be related to metastasis and poor prognosis in lung cancer

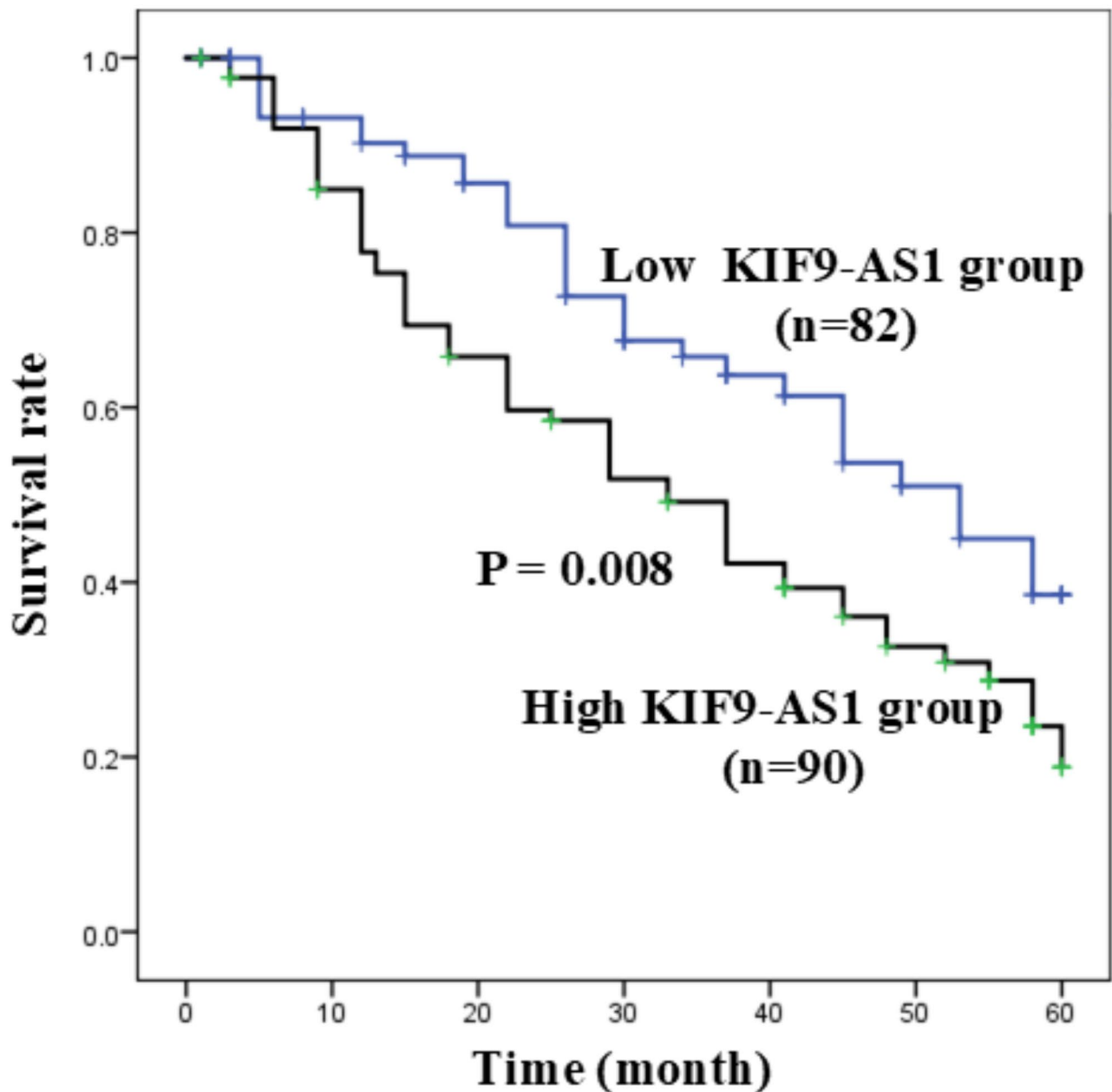


Fig. 4 The prognosis significance of lncRNA KIF9-AS1. Kaplan-Meier curves for malignant PN patients. The survival rate in low KIF9-AS1 group was higher than that in high KIF9-AS1 group

[26]. Here, we found that the KIF9-AS1 presented high sensitivity and specificity in distinguishing malignant PN from benign PN, especially combined with computed tomography (CT), which highlighted the possibility that KIF9-AS1 was associated with the deterioration of PN. Subsequent regression analysis also proved that KIF9-AS1 was a risk factor for malignant PN. Our 5-year follow-up in patients showed that compared with the benign PN group, the survival rate in malignant PN group with abnormally elevated KIF9-AS1, was significantly reduced. Multivariate Cox regression

analysis demonstrated that in addition to KIF9-AS1, nodule diameter was also a risk factor of malignant PN. In previous study, the nodule size has been proved as a factor that can not be ignored for lung cancer [5, 27]. We obtained similar results to previous studies.

Our study also has some limitations. For instance, the above findings still need to be verified in cell models or animal models and these model may involve effects on cell proliferation, migration and apoptosis, underlying signaling pathways and epigenetics. We expect to elucidate them in our future work.

Table 2 Multivariate Cox regression analysis of risk factors in patients with malignant PNs

Variables	Multivariate analysis		
	HR	95% CI	P value
Age	1.209	0.789–1.853	0.382
gender	0.970	0.619–1.522	0.896
Smoking history	1.184	0.662–2.118	0.569
Extra-lung cancer history	1.073	0.643–1.790	0.787
Family cancer history	1.026	0.538–1.956	0.938
Nodule density	0.733	0.476–1.128	0.158
Air bronchogram	1.421	0.884–2.284	0.147
Nodule diameter	1.642	1.032–2.613	0.036
LncRNA KIF9-AS1	1.805	1.141–2.855	0.012

Note: HR, hazard ratio, CI, confidence interval, PNs, pulmonary nodules

Conclusions

Collectively, KIF9-AS1 was significantly elevated in malignant PNs compared to the benign PNs. The expression of KIF9-AS1 was positively associated with tumor markers CEA and CYFRA21-1. Assessment of serum KIF9-AS1 level contributed to clinical diagnosis and prognosis of malignant PNs. It is expected that our findings can provide a theoretical reference for the diagnosis of benign and malignant PNs and the determination of therapeutic targets.

Abbreviations

PNs	Pulmonary nodules
ROC	Receiver operator characteristic
CEA	Carcinoembryonic antigen
CT	Computed tomography
LncRNA	Long non-coding RNAs
NSCLC	Non-small cell lung cancer
NC	Nasopharyngeal carcinoma
NSE	Neuron-specific enolase

Acknowledgements

None.

Author contributions

Junying Zhao, Zhongjun Jing and Laichong Huang carried out the concepts, design and definition of intellectual content, Laichong Huang, Huichao Wu, Jian Liu, Zihua Qi and Xianjun Ma provided assistance for data acquisition, data analysis and statistical analysis. All authors performed the experiment, and draft of the manuscript. Huichao Wu, Jian Liu and Laichong Huang revised the manuscript critically for important intellectual content. All authors have read and approved the content of the manuscript.

Funding

This study was funded by Beijing Chao En Xiang Inheritance of traditional Chinese Medicine Development Foundation 2023 "Stepping into a New Horizon" Research Project— An Analysis of National Chinese Medicine Master Chao Enxiang's Clinical Experience in Applying the Tonifying the Lung and Activating the Spleen Method in the Treatment of Chronic Pulmonary Diseases (2023CC04).

Data availability

The datasets used and/or analysed during the current study are available from the corresponding author on reasonable request.

Declarations

Ethics approval and consent to participate

This study obtained the approval of the Ethics Committee of Hospital of University of Jinan and informed consent of all enrolled patients.

Consent for publication

Not applicable.

Competing interests

The authors declare no competing interests.

Received: 5 November 2024 / Accepted: 6 April 2025

Published online: 09 May 2025

References

- Tanner NT, Aggarwal J, Gould MK, Kearney P, Diette G, Vachani A, et al. Management of pulmonary nodules by community pulmonologists: A multicenter observational study. *Chest*. 2015;148(6):1405–14. PubMed PMID: 26087071. Pubmed Central PMCID: PMC4665735. Epub 2015/06/19.
- Wang Y, Jing L, Liang C, Liu J, Wang S, Wang G. Comparison of the safety and effectiveness of the four-hook needle and Hook wire for the preoperative positioning of localization ground glass nodules. *J Cardiothorac Surg*. 2024;19(1):35. PubMed PMID: 38297385. Pubmed Central PMCID: PMC10829251. Epub 2024/02/01.
- Liu HY, Zhao XR, Chi M, Cheng XS, Wang ZQ, Xu ZW, et al. Risk assessment of malignancy in solitary pulmonary nodules in lung computed tomography: a multivariable predictive model study. *Chin Med J (Engl)*. 2021;134(14):1687–94. PubMed PMID: 34397595. Pubmed Central PMCID: PMC8318662. Epub 2021/08/17.
- Henschke CI, Yankelevitz DF, Mirtcheva R, McGuinness G, McCauley D, Miettinen OS, et al. CT screening for lung cancer: frequency and significance of part-solid and nonsolid nodules. *AJR Am J Roentgenol*. 2002;178(5):1053–7. PubMed PMID: 11959700. Epub 2002/04/18.
- Larici AR, Farchione A, Franchi P, Ciliberto M, Cicchetti G, Calandriello L et al. Lung nodules: size still matters. *Eur Respir Rev*. 2017;26(146). PubMed PMID: 29263171. Pubmed Central PMCID: PMC9488618. Epub 2017/12/22.
- Li Z, Xu W, Gu T, Cao X, Wu W, Chen L. Tumor size, but not consolidation-to-tumor ratio, is an independent prognostic factor for part-solid clinical T1 non-small cell lung cancer. *Thorac Cancer*. 2023;14(6):602–11. PubMed PMID: 36578128. Pubmed Central PMCID: PMC9968594. Epub 2022/12/30.
- Bray F, Ferlay J, Soerjomataram I, Siegel RL, Torre LA, Jemal A. Global cancer statistics 2018: GLOBOCAN estimates of incidence and mortality worldwide for 36 cancers in 185 countries. *CA Cancer J Clin*. 2018;68(6):394–424. PubMed PMID: 30207593. Epub 2018/09/13.
- Sicular S, Alpaslan M, Ortega FA, Keathley N, Venkatesh S, Jones RM et al. Reevaluation of missed lung cancer with artificial intelligence. *Respir Med Case Rep*. 2022;39:101733. PubMed PMID: 36118268. Pubmed Central PMCID: PMC9472074. Epub 2022/09/20.
- Li H, Li M, Guo H, Lin G, Huang Q, Qiu M. Integrative analyses of Circulating mRNA and LncRNA expression profile in plasma of lung cancer patients.

- Front Oncol. 2022;12:843054. PubMed PMID: 35433477. Pubmed Central PMCID: PMC9008738. Epub 2022/04/19.
10. Chen X, Zhu X, Yan W, Wang L, Xue D, Zhu S, et al. Serum LncRNA THRIL predicts benign and malignant pulmonary nodules and promotes the progression of pulmonary malignancies. *BMC Cancer*. 2023;23(1):755. PubMed PMID: 37582734. Pubmed Central PMCID: PMC10426220. Epub 2023/08/16.
 11. Zhang H, Wang SQ, Zhu JB, Wang LN, Lin H, Li LF, et al. LncRNA CALML3-AS1 modulated by m(6)A modification induces BTNL9 methylation to drive non-small-cell lung cancer progression. *Cancer Gene Ther*. 2023;30(12):1649–62. PubMed PMID: 37884580. Epub 2023/10/27.
 12. Jiang N, Meng X, Mi H, Chi Y, Li S, Jin Z, et al. Circulating LncRNA XLOC_009167 serves as a diagnostic biomarker to predict lung cancer. *Clin Chim Acta*. 2018;486:26–33. PubMed PMID: 30025752. Epub 2018/07/22.
 13. Yu Y, Lu X, Yan Y, Wang Y, Meng J, Tian S et al. The LncRNA KIF9-AS1 accelerates hepatocellular carcinoma growth by recruiting DNMT1 to promote RAI2 DNA methylation. *J Oncol*. 2022;2022:3888798. PubMed PMID: 36276278. Pubmed Central PMCID: PMC9584731. Epub 2022/10/25.
 14. You H, Wang S, Yu S. KIF9-AS1 promotes nasopharyngeal carcinoma progression by suppressing miR-16. *Oncol Lett*. 2020;20(5):241. PubMed PMID: 32973955. Pubmed Central PMCID: PMC7509506. Epub 2020/09/26.
 15. Jin Y, Huang R, Xia Y, Huang C, Qiu F, Pu J, et al. Long noncoding RNA KIF9-AS1 regulates transforming growth Factor-beta and autophagy signaling to enhance renal cell carcinoma chemoresistance via microRNA-497-5p. *DNA Cell Biol*. 2020;39(7):1096–103. PubMed PMID: 32343913. Epub 2020/04/29.
 16. Chen S, Harmon S, Perk T, Li X, Chen M, Li Y, et al. Using neighborhood Gray tone difference matrix texture features on dual time point PET/CT images to differentiate malignant from benign FDG-avid solitary pulmonary nodules. *Cancer Imaging*. 2019;19(1):56. PubMed PMID: 31420006. Pubmed Central PMCID: PMC6697997. Epub 2019/08/20.
 17. Liu M, Li W, Song F, Zhang L, Sun X. Silencing of LncRNA MIAT alleviates LPS-induced pneumonia via regulating miR-147a/NKAP/NF-kappaB axis. *Aging*. 2020;13(2):2506–18. PubMed PMID: 33318298. Pubmed Central PMCID: PMC7880384. Epub 2020/12/16.
 18. Xing C, Sun SG, Yue ZQ, Bai F. Role of LncRNA LUCAT1 in cancer. *Biomed Pharmacother*. 2021;134:111158. PubMed PMID: 33360049. Epub 2020/12/29.
 19. Yao J, Gao R, Luo M, Li D, Guo L, Yu Z, et al. Long noncoding RNA KIF9-AS1 promotes cell apoptosis by targeting the microRNA-148a-3p/suppressor of cytokine signaling axis in inflammatory bowel disease. *Eur J Gastroenterol Hepatol*. 2021;33(1S Suppl 1):e922–32. PubMed PMID: 34750325. Pubmed Central PMCID: PMC8734634. Epub 2021/11/10.
 20. Grunnet M, Sorensen JB. Carcinoembryonic antigen (CEA) as tumor marker in lung cancer. *Lung Cancer*. 2012;76(2):138–43. PubMed PMID: 22153832. Epub 2011/12/14.
 21. Li C, Liu L, You R, Li Y, Pu H, Lei M, et al. Trajectory patterns and cumulative burden of CEA during follow-up with non-small cell lung cancer outcomes: A retrospective longitudinal cohort study. *Br J Cancer*. 2024;130(11):1803–8. PubMed PMID: 38594371. Pubmed Central PMCID: PMC11130257. Epub 2024/04/10.
 22. Ajona D, Ramirez A, Sainz C, Bertolo C, Gonzalez A, Varo N, et al. A model based on the quantification of complement C4c, CYFRA 21–1 and CRP exhibits high specificity for the early diagnosis of lung cancer. *Transl Res*. 2021;233:77–91. PubMed PMID: 33618009. Pubmed Central PMCID: PMC8931205. Epub 2021/02/23.
 23. Okamura K, Takayama K, Izumi M, Harada T, Furuyama K, Nakanishi Y. Diagnostic value of CEA and CYFRA 21–1 tumor markers in primary lung cancer. *Lung Cancer*. 2013;80(1):45–9. PubMed PMID: 23352032. Epub 2013/01/29.
 24. Yuan J, Sun Y, Wang K, Wang Z, Li D, Fan M, et al. Development and validation of reassigned CEA, CYFRA21-1 and NSE-based models for lung cancer diagnosis and prognosis prediction. *BMC Cancer*. 2022;22(1):686. PubMed PMID: 35729538. Pubmed Central PMCID: PMC9214980. Epub 2022/06/22.
 25. Yang Q, Wang M, Xu J, Yu D, Li Y, Chen Y, et al. LINC02159 promotes non-small cell lung cancer progression via ALYREF/YAP1 signaling. *Mol Cancer*. 2023;22(1):122. PubMed PMID: 37537569. Pubmed Central PMCID: PMC10401734. Epub 2023/08/04.
 26. Loewen G, Jayawickramarajah J, Zhuo Y, Shan B. Functions of LncRNA HOTAIR in lung cancer. *J Hematol Oncol*. 2014;7:90. PubMed PMID: 25491133. Pubmed Central PMCID: PMC4266198. Epub 2014/12/11.
 27. Autotransfusion machines. *Health Devices*. 1988;17(12):371. PubMed PMID: 3273932. Epub 1988/12/01.

Publisher's note

Springer Nature remains neutral with regard to jurisdictional claims in published maps and institutional affiliations.